A surface forces platform for dielectric measurements

Yoon-Kyoung Cho and Steve Granick

Citation: The Journal of Chemical Physics **119**, 547 (2003); doi: 10.1063/1.1568931

View online: http://dx.doi.org/10.1063/1.1568931

View Table of Contents: http://scitation.aip.org/content/aip/journal/jcp/119/1?ver=pdfcov

Published by the AIP Publishing

A surface forces platform for dielectric measurements

Yoon-Kyoung Cho[a] and Steve Granick
Department of Materials Science and Engineering, University of Illinois, Urbana, Illinois 61801

(Received 1 November 2002; accepted 28 February 2003)

Methods are described to implement dielectric spectroscopy (frequency range 10^{-1}–10^{6} Hz) within a surface forces apparatus by using as electrodes silver sheets on the backside of mica. These methods are applied to study the competitive effects of surface alignment, confinement, and shear field on 5CB (5-cyanobiphenyl), a nematic liquid crystal at the experimental temperature of 25 °C. In the planar orientation, films could be squeezed to a minimum thickness of ≈5 Å, the molecule's thickness. In the perpendicular (homeotropic) orientation, films could be squeezed to ≈25 Å, the expected thickness of the head-to-tail 5CB dimer. It was difficult to discuss responses at $f > 10^{5}$ Hz quantitatively because the peak was not visible in the experimental frequency window. Nonetheless, the onset of the relaxation mode for the planar oriented molecules appears at higher frequency than for the homeotropic orientation. A slower relaxation mode, peaked at $f \approx 10$ Hz, was assigned to electrode polarization due to the mobility of trace ions within the 5CB samples although these samples were >99.7% pure. The peak frequency was a factor of 3 slower with homeotropic than planar alignment and, in both cases, independent of film thickness except when the film thickness exceeded 10 μm. This was explained using a simple model based on the assumption that trace ions move to oppositely charged electrodes to form electric double layers. A small influence of shear on the dielectric response was observed but only when the dielectric response was measured at the same frequency as the large-amplitude shear deformation. Also described is the use of capacitance to measure force–distance profiles. © *2003 American Institute of Physics.*
[DOI: 10.1063/1.1568931]

I. INTRODUCTION

The influence of confinement on the structure of thin liquid films and their dynamical responses to external fields lies at the heart of many fundamental issues in nature and technology. These include applications as diverse as adhesion, colloidal stability, lubrication, and liquid crystal display technology. Differences between thin and thick films are manifest in all of these areas, especially strikingly so in the case of ordered thin films of liquid crystals. On the scientific side, liquid crystals present intriguing systems because surface-induced order is so prominent. There is also technological motivation when one considers the liquid crystal materials have wide application in electric-field-driven display devices.

The goal of this study was to adapt the surface forces apparatus (SFA) for dielectric measurements. The large impact of the SFA in thin film studies[1,2] can be traced to its convenience in varying film thickness between atomically-smooth surfaces from macroscopic separations down to separations as small as a few nanometers or even angstroms. The surface forces apparatus and its modifications for shear measurement[3] have been used extensively to investigate static forces (equilibrium interactions between surfaces, especially surfaces separated by liquids) and time or frequency-dependent properties (the dynamic viscosity) of fluids confined between solid surfaces. Applied to liquid crystals, these SFA techniques have been used to study a variety of subjects involving nematic liquid crystals. These include force-distance relations of confined liquid crystals,[4–6] especially as they depend on the relative orientation of the confining mica surfaces, and recently their linear and nonlinear shear rheology (including stick-slip transitions) as a function of relative orientation of the confining mica crystals.[6–8]

It is desirable to develop additional experimental techniques, with which to complement the information gained from force-based measurement. Safinya and co-workers have investigated the structure and orientation of oriented liquid crystals using synchrotron x-ray scattering within a modified SFA but those experiments have been limited, to date, to film thickness 0.1 μm or larger.[9,10] Recently we described the use of time-resolved Fourier transform infrared spectroscopy (TRS-FTIR) to probe the dynamic structure of confined fluids[11] and this technique was applied to study the same experimental system as this study,[12] but those experiments, to date, have been limited to micrometer-thick films.

Effects of confinement on liquid crystals confined to lesser thickness have previously been studied using dielectric spectroscopy by introducing the liquid crystal into porous glasses with pore diameter as small as a few nanometers.[13] Those studies show that the phase transition from the isotropic to nematic state is, in pores, significantly depressed and more gradual than in the bulk state. However, the randomness of pore sizes and the roughness of pore surfaces might have complex effects on molecular ordering in a confined geometry comprised of pores. In addition, the randomness of

[a]Present address: Biochip Project Team, Samsung Advanced Institute of Technology, Suwon, 440-600, Republic of Korea.

pore geometry implies that electric field cannot be applied at a definite angle relative to the molecular orientation of the liquid crystal.

In the bulk state, dielectric properties of nematic liquid crystals have been studied extensively.[14,15] Direct information on molecular orientation is given by relaxations attributable to orientational polarizability, commonly observed at frequencies higher than MHz. It is also known, though less studied, that liquid crystals also commonly exhibit a low-frequency dielectric dispersion, believed to result from impurity ions present in trace amounts in commercially available liquid crystalline materials.[16,17] Ionic impurities may cause damage in commercial liquid crystal display (LCD) applications.[16,17]

Here we describe what we believe to be the first application of dielectric spectroscopy to nanometer-thin films within a SFA. The system is the nematic liquid crystal, 4-*n*-pentyl-4′-cyanobiphenyl, customarily abbreviated 5CB. This molecule is also known as 5-cyanobiphenyl. 5CB is known to have a nematic phase between 24.0 and 35.3 °C. Its physical properties have been studied extensively.[14,15,18,19] The dielectric anisotropy $\Delta\varepsilon$ of 5CB is positive because the dipole moment of the cyano group in the molecule is nearly parallel to the long molecular axis. We focus on confinement-induced changes of dielectric response and are interested especially in its dependence on film thickness, shear, and orientation of the liquid crystal molecules parallel or perpendicular to the confining surfaces.

Force–distance relations of the similar 8CB system are known.[4,5,7,8] This laboratory has described elsewhere the force–distance relations for 5CB, with special attention given to the accompanying shear response, in the case of planar alignment, as a function of relative twist angle between the confining mica lattices.[6]

II. EXPERIMENT

A. SFA setup for dielectric measurements

A surface forces apparatus (SFA) modified for dynamic oscillatory shear[20] was the experimental platform. In this technique, two sheets of muscovite mica are cleaved to be 2–4 μm thick and atomically smooth over an area of $\sim$1 cm^2. They are glued onto cylindrically-shaped lenses with radius of curvature $R\sim 2$ cm and oriented in a crossed-cylinder configuration. It is routine, in the SFA technique, to coat the backside of the mica sheets with silver so that the surface separation may be determined using multiple beam interferometry.[1] We find it convenient to employ silver films 660 Å thick, deposited by vacuum sputtering. As we now describe, these silver films are continuous and can be employed as electrodes for dielectric measurement of samples between the intervening mica sheets.

Since stray capacitance from wires or screws can easily overwhelm the response from the interesting sample, electrical connection was made directly to each of the silvered sides of the mica using silver-containing epoxy (EPO-TEK 415G, Epoxy Technology, Inc.). After application, this was dried overnight under purge with dry N_2 gas. During subsequent experiments, a dry atmosphere was maintained by placing P_2O_5 within the sealed sample chamber.

The steel outer chamber of the SFA served as a convenient Faraday box. No shielding was given to the wire that was glued to the silvered mica, but the length of this wire was less than 1 cm. Except for this, all other wires were shielded (regular BNC cables) and the total length of wire to the dielectric analyzer was less than 30 cm.

Dielectric data were acquired using a Solartron 1260 Gain-Phase Impedance Analyzer connected to a Solartron 1296 Dielectric Interface. The nominal frequency range of this apparatus is 10^{-4}–10^{7} Hz but our experiments were usually performed in the range 10^{-1}–10^{6} Hz. At lower frequency a prohibitively long time is needed to acquire data and there is risk that dc conductivity of polar impurities would overwhelm the sample response. At higher frequency, the signals were found to be too noisy. In all measurements, the applied ac field was 0.1 V_{RMS}. This input voltage is small when one considers the large voltage drop across the intervening mica. When the sample thickness is 10 Å, and the mica thickness is 2 μm, for example, the voltage drop across the sample typically is a fraction $\approx 10^{-1}$ to 10^{-3} of the input voltage, depending on the sample's resistivity.

The liquid crystal was purchased from BDH Corp. (purity >99.7%) and used without further purification. The length of a single molecule in the long axis is 18.7 Å. However, 5CB molecules associate head-to-tail to form dimers whose thickness is estimated to be 25 Å.[6,18] The static dielectric constant of 5CB is known as 19.7 for $\varepsilon_{\parallel}$ and 6.7 for $\varepsilon_{\perp}$.[14]

All measurements were performed in a temperature-controlled room thermostatted at 25 °C. Surface separation was measured either by multiple beam interferometry or by capacitance. Repeated measurements at the same surface separation showed essentially identical results.

B. Data analysis

When surface force is measured in the crossed-cylinder geometry, its integration over the many distances of separation gives, by the well-known Derjaguin approximation,[1] a force that is proportional to the energy of interaction between two flat and parallel surfaces separated by the same distance of closest approach. A similar argument can be applied to dielectric measurements (the integral of electric field being electric potential). However to do this requires knowing the precise size and location of the droplet-sized sample located between the surfaces, which is troublesome, and this was not done.

A schematic diagram of the geometry for dielectric measurement within a SFA is shown in Fig. 1. One sees the crossed-cylinder geometry of a SFA, which is equivalent in projection to a sphere-on-flat geometry. The spherical curvature meets the opposed surface in a proximal zone of closest confinement (zone I) and a second distal zone (zone II). The serial result of the dielectric constant of mica (ε_M) and of liquid crystal sample ($\varepsilon^*_{\mathrm{LC}}$) produces the detected capacitance, C^*. The C^* is a complex quantity with real and imaginary components and depends on frequency. In response to an ac drive electric field at frequency ω, the dielec-

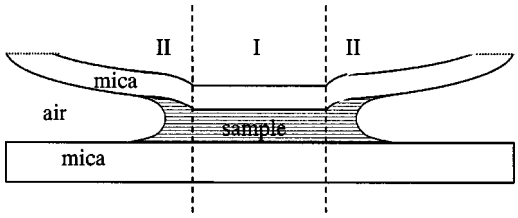

FIG. 1. Geometry for dielectric measurements within a surface forces apparatus (SFA). The sketch shows the crossed-cylinder geometry of a SFA, which is equivalent in projection to a sphere-on-flat geometry. The mica sheets separated by a droplet of nematic liquid crystal come into contact where the spherical curvature meets the proximal opposed surface (zone I). A second distal zone (zone II) includes thicker portions of the droplet and also ambient gas within the measurement chamber. The backside of each mica sheet is coated by a silver electrode, to which ac or dc voltage is applied. The serial combination of the dielectric constant of mica (ε_m) and liquid crystal sample (ε^*_{LC}) produces the detected frequency-dependent capacitance: a complex number.

tric constant can be represented as having one component in phase, $C'(\omega)$, and a second component out of phase, $C''(\omega)$,

$$C^*(\omega)=C'(\omega)-i^*C''(\omega). \tag{1}$$

It proved impossible to unambiguously separate $C'(\omega)$ of the mica from the total $C'(\omega)$ (mica plus sample), although many attempts to perform this exercise were attempted. Therefore the frequency dependence of the sample's dielectric constant could not be separated from that of the measurement cell. A detailed analysis of the information that would be required to perform the unambiguous separation is presented by us elsewhere.[21] We consider here therefore only the imaginary part of the capacitance, $C''(\omega)$. Because the dielectric loss within the mica is negligibly small, this has the same frequency dependence as the dielectric loss, $\varepsilon''(\omega)$.

III. RESULTS AND DISCUSSION

A. Alignment of 5CB in homeotropic and planar orientation

Homeotropic alignment is favored when the surface is hydrophobic, especially when there is no preferential orientation or roughness on the surface.[4] One common way to induce the homeotropic orientation is to allow adsorption of a lecithin or surfactant monolayer to render the surface hydrophobic.[22] However, we accidentally found out that homeotropic orientation resulted when the mica was exposed overnight to silver-containing epoxy (used to make electrical connections, as described in the Experiment) during the time that it dried. Force–distance profiles of the surfaces modified in this way showed an adhesive contact and the hard wall thickness was minimal (<2 Å). Repeated experiments showed the same results and we accepted it as a simple way of inducing homeotropic orientation. Dielectric measurement with mica surface only (either prior to or after surface modification) showed the same results. We believe the surface modification originated from the organic vapor that came from the epoxy setting.

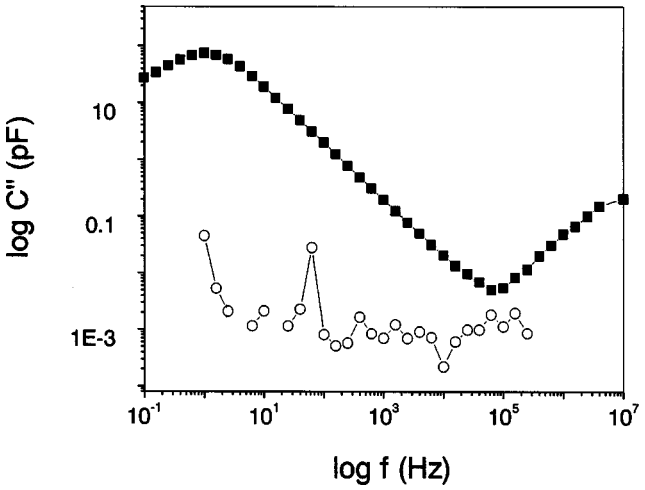

FIG. 2. Control experiment showing the small relative contribution of the measurement cell to the dielectric response. The out-of-phase capacitance, $C''(f)$, is plotted on log–log scales against a frequency of ac voltage (f) for mica sheets in van der Waals contact in air (circles) and for mica sheets separated by a sample of 5CB nematic liquid crystal of bulk thickness and aligned in the homeotropic orientation (squares). The loss peak in the low frequency regime (10^{-1}–10^3 Hz) is attributed to the Maxwell–Wagner polarization which is closely related to the conductivity of the sample. The upturn of dielectric loss at the highest frequencies is attributed to the onset of a loss peak stemming from molecular flip of liquid crystal molecules.

When seeking to avoid this effect and to produce the planar orientation, a careful procedure of cleaving and gluing the mica was used to align two freshly-cleaved mica sheets in their original crystallographic direction. The 5CB sample was then introduced between the surfaces to produce a planar orientation before the drying procedure of setting silver-containing epoxy was initiated. To determine the orientation of the nematic director relative to the surface, we used the method of Ruths *et al.*,[7] which is based on analyzing the sample's birefringence. Birefringence shows up directly when one uses multiple beam interferometry to measure silver–silver separation within a surface forces apparatus; each order fringe appears at two wavelengths. In brief, when 5CB was in planar orientation (aligned parallel to the mica surfaces), the extraordinary or "γ" fringes, which appear at longer wavelength, appear to move faster than the ordinary "β" fringes as the surface separation, D, is increased. Therefore, it appears that the β–γ fringe splitting increases when D increases. On the other hand, in the homeotropic orientation where the nematic director is perpendicular to the surface, the medium is isotropic to the light that passes normally through the surfaces. Therefore in this alignment, the β–γ fringe splitting decreases as D increases, as is normally seen in isotropic media.

B. Orientational and thickness dependence of dielectric loss at $f<10^5$ Hz

Since the measurement represents the serial combination of sample and mica, it is important to validate that the response of mica is negligible in its effect on the out-of-phase capacitance, $C''(\omega)$, the loss response, upon which we focus in this study. In Fig. 2, the loss response of the sample-free cell with mica sheets in adhesive contact in air is plotted

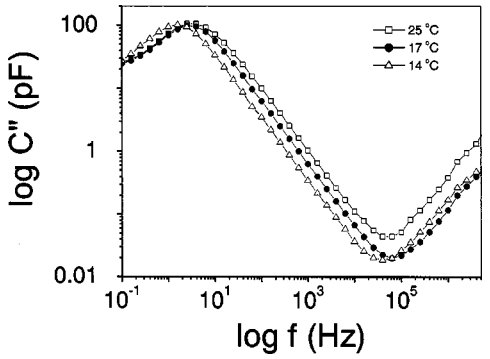

FIG. 3. Dielectric responses of 5CB confined to 27 Å within a SFA. Measurements were done at 25 °C (squares), 17 °C (circles), and 14 °C (triangles). Temperature dependent shift of the Maxwell–Wagner polarization peak (10^{-1}–10^{3} Hz) is clearly visible. In contrast, only a portion of the dielectric loss located at higher frequencies is observed and the temperature dependence of the peak is not clearly shown.

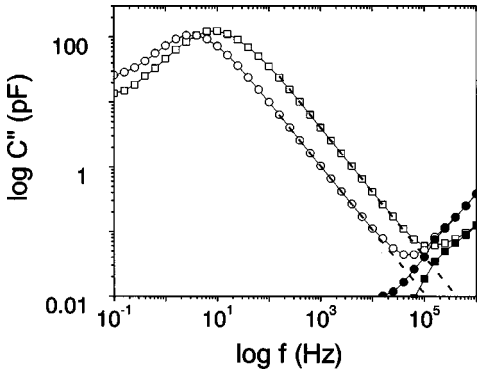

FIG. 4. Comparison of 5CB dielectric responses for ultrathin films in the homeotropic (circles, a film 27 Å thick) and planar (squares, a film 5 Å thick) orientations. The out-of-phase capacitance, $C''(f)$, is plotted on log–log scales against ac frequency (f). Dashed line is the contribution of the dc conductivity and closed symbols denote the dielectric loss of 5CB after subtraction of the dc conductivity.

against frequency on log–log scales. The measurement shows no dependence on frequency. Its magnitude is on the order of the apparatus sensitivity, 10^{-14}–10^{-15} F. The data obtained in the presence of the 5CB sample are orders of magnitude larger than this.

The loss peak in the low frequency regime (10^{-1}–10^{3} Hz) is attributed to the *Maxwell–Wagner* polarization, which is also called *charge-carrier relaxation*. Liquid crystal samples contain charge carriers which can be moved by electric forces between polarized walls. This process is rate-limited by diffusion and as it is closely related to the conductivity; it is also named *conductivity relaxation*. The relaxation time τ_c of a conductivity relaxation is given by

$$\tau_c = \varepsilon_0 \varepsilon_r / \sigma_{\mathrm{dc}}, \tag{2}$$

where σ_{dc} is the dc conductivity of the material, ε_0 is the permittivity of free space, and ε_r is the relative permittivity of the material.

The upturn of dielectric loss at the highest frequencies is attributed to the onset of a loss peak stemming from molecular flip of liquid crystal molecules. Only a portion of the relaxation mode is evident, beginning at frequencies above 10^5 Hz. This peak generally agrees with expectations from the literature, where relaxation modes with peak frequency in the 10 MHz range are assigned to the flip and tumbling motions of individual liquid crystal molecules.[23,24] This relaxation is discussed in the following section.

In order to validate that these two distinct peaks are relaxation processes, temperature was varied. Figure 3 shows the dielectric responses of 5CB confined to 27 Å within a SFA. Measurements were done at 25 °C, 17 °C, and 14 °C. The temperature of the thermostatted room, in which these measurements were performed, had to be equilibrated for several hours at each new temperature. Thus, it was not convenient to lower the temperature sufficiently to observe significant shifts of the molecular relaxation peaks. Nonetheless, shifts of the Maxwell–Wagner polarization peak (10^{-1}–10^{3} Hz) are clearly visible. In contrast, the peak located at higher frequencies is not visible in the experimental frequency window and thus temperature dependence of this peak was not observed. However, separate experiments done in a dielectric measurement setup outside the SFA (Ref. 21) and also literature values[23,24] suggest that this peak is also a relaxation process.

Figure 4 compares the dielectric responses of 5CB in the homeotropic and planar orientations when squeezed to their minimum thickness. The measured minimum thickness is as expected from the alignment inferred from optical birefringence. For planar orientation it is 5 Å, consistent with the thickness of a single 5CB molecule. For homeotropic orientation it is 27 Å, close to the 25 Å expected from head-to-tail dimer formation.[6,18]

The position of the interfacial polarization peak centered at ≈10 Hz was a factor of 3 slower when the molecules had homeotropic rather than planar orientation. This anisotropy of the conductivity relaxation time stems from the anisotropy of dielectric permittivity as well as anisotropy of the conductivity as noted in Eq. (2). In addition, the difference of surface chemistry depending on the alignment may also result in the orientational anisotropy.

Figure 5 (top panel) compares, at various film thicknesses from 5 Å to 194 μm, the loss dielectric response of 5CB in the planar orientation. On logarithmic scales the slope of $\log C''$ plotted against $\log f$ was 0.66 for $f < f_{\mathrm{peak}}$ and 1.0 for $f > f_{\mathrm{peak}}$, signifying a broad distribution of relaxation times at the lower frequencies. These slopes did not change with film thickness. The peak intensity increases with decreasing thickness because capacitance increases. Similar experiments were also performed with samples having the homeotropic orientation as shown in Fig. 5 (bottom panel).

Even at the largest surface separations, domains of different director directions were not observed. Such domains would have been obvious, if present, from the optical interference pattern as light passed through the interferometer formed by the opposed back-silvered mica sheets. Domains would result in discontinuous interference fringes.[6,7]

In Fig. 6, the conductivity relaxation time, which is defined as the inverse peak frequency, is plotted against film thickness on log–log scales. More data are shown than were included in the traces of Fig. 5. Two interesting observations

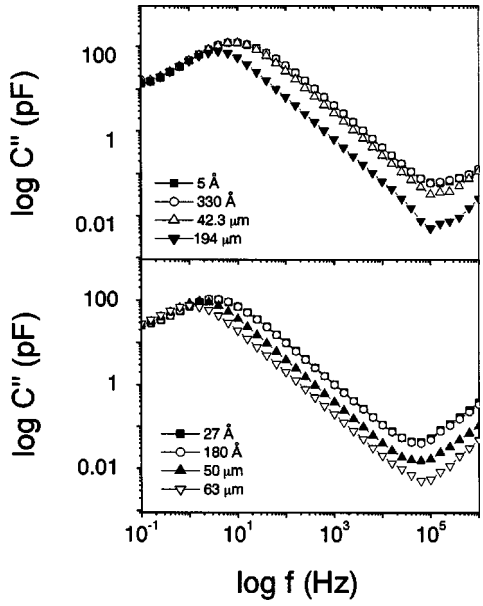

FIG. 5. Thickness dependence of the frequency-dependent dielectric response for 5CB in the planar orientation (top panel) and the homeotropic orientation (bottom panel). The out-of-phase capacitance, $C''(f)$, is plotted on log–log scales against ac frequency (f). Note that the intensity increases with diminishing film thickness because the capacitance increases. The peak in the low frequency regime, attributed to ion conductivity, shifted to higher frequency as the film thickness decreased. In the top panel, the film thickness was 194 μm (filled triangles), 42.3 μm (open triangles), 330 Å (open circles), and 5 Å (filled squares). In the bottom panel, the film thickness was 63 μm (open triangles), 50 μm (filled triangles), 180 Å (open circles), and 27 Å (filled squares). Data taken at other values of film thickness are omitted for clarity but summarized in Fig. 6.

may be made. First, this average relaxation time decreased with decreasing film thickness for films whose thickness exceeded about 10 μm, but became roughly constant at lesser thickness. Second, this relaxation time was slower when the film had a homeotropic rather than planar orientation.

As noted previously, orientational anisotropy of conductivity relaxation time may be the consequence of the anisotropies of permittivity and conductivity as well as the difference in surface chemistry. The conductivity relaxation time, related to the electrode polarization, is an interfacial

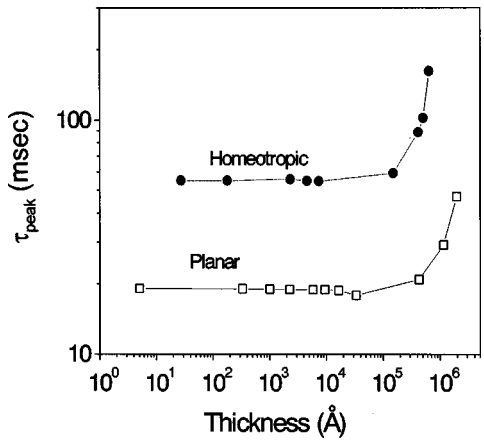

FIG. 6. The conductivity relaxation time, $\tau_{peak} \equiv 1/2\pi f_{max}$, is plotted on log–log scales against film thickness for films of homeotropic (circles) and planar orientation (squares).

phenomena and therefore one may not expect to see any dependence on the film thickness. But, in Fig. 6, the sudden onset of this striking change of thickness dependence calls for an additional explanation.

As summarized in Ref. 17, Imai *et al.* studied the influence of ion conduction on the viscosity of 5CB; Colpaert *et al.* suggested that studying the behavior of ions under electric fields is a good way to characterize trace amounts of ions in liquid crystals materials; Murakami *et al.* measured the mobility of ions in 5CB from transient photocurrent experiments with bulk thickness of liquid crystal samples and attributed it to the formation of the Helmholtz double layer.[17] They could also estimate important ion parameters such as ion mobility and concentration using a simple model assuming that an ion sheet oscillates between two parallel plates under an ac field.[17] We note parenthetically that it is less likely that the peak at ~10 Hz originated from the potassium ions dissolved from mica surfaces. First of all, nematic liquid crystals always contain impurity ions as pointed out by the various research groups just cited. Second, separate experiments with Ge surfaces showed similar results (Y.-K. Cho, Ph.D. thesis, University of Illinois at Urbana-Champaign).

Ion velocity, $2Df_{peak}$, can be expressed roughly as $2Df_{peak} = \mu E = \mu V_{RMS}/D$. Therefore the ion mobility is

$$\mu = \frac{2D^2 f_{peak}}{V_{RMS}}, \tag{3}$$

where D is film thickness, f_{peak} is the peak frequency of electrode polarization peak, μ is the ion mobility, V_{RMS} is the root-mean-square applied voltage, and E is the electric field applied.

At the larger levels of film thickness, ions move more slowly than the applied ac field and the measured relaxation reflects diffusion of ions across the gap during the period of the oscillation. Eventually, ions diffuse fast enough to reach the oppositely charged surface during the period of an oscillation, thus forming an electric double layer. In this interpretation, the ion mobility would be $\mu = D_{crit}/\tau_c^* E$ (D_{crit} is the critical film thickness for onset of frequency independence and E is the applied electric field, V_{RMS}/D_{crit}). In this regime, the liquid crystal layer is more conductive than the electric double layer and almost the entire voltage is applied to the electric double layer. The capacitance then reflects mainly ions within the double layer whose thickness is about the size of the ions and independent of film thickness.

Because the voltage, 0.1 V_{RMS}, was applied to the silver electrodes located at the backsides of mica sheets of thickness ≈ 3 μm, the exact voltage applied between the mica surfaces and not lost within the mica itself in the cross-cylinder geometry is difficult to estimate. Efforts to estimate the real voltage between mica surfaces using impedance measurements failed because the contact area was different in every measurement due to the cross-cylinder geometry surfaces. Therefore, the ion mobility estimated from the above argument, normalized by the applied voltage, then takes the values $\mu/V_{RMS} = 2.5 \times 10^{-4}$ cm^2/s and 3.7×10^{-3} cm^2/s for the homeotropic and planar orientations, respectively.

C. Orientational dependence of molecular relaxation at $f > 10^5$ Hz

The peak of the dielectric loss at $f > 10^5$ Hz is not visible in the experimental frequency window. From literature, in planar orientation, the dielectric loss at $f > 10^5$ Hz corresponds to the transverse component of the dielectric constant, $\varepsilon_{\perp}^{*}$, because the director of the molecules is perpendicular to the electric field. This relaxation mode reflects a process whose peak is about two orders of magnitude faster than when the molecules are oriented in the same direction as the electric field (homeotropic orientation). It stems from tumbling of the molecular long axis around the local director. On the other hand, the slower process that results in $\varepsilon_{\parallel}^{*}$ in the homeotropic orientation has been assigned to molecular flip about the short axis.[23,24]

The out-of-phase capacitance of the dielectric medium containing free-ionic charges would be written as

$$C''(\omega) \propto \varepsilon''(\omega) + \sigma_{\mathrm{dc}}/\omega\varepsilon_0, \tag{4}$$

where σ_{dc} is the dc conductivity due to the free-ionic charges. In Fig. 4, the dashed line is the contribution of the dc conductivity effect and closed symbols denote the dielectric loss of 5CB after subtraction of the dc conductivity. Since our available frequency range ends at 1 MHz it is difficult to discuss responses at these frequencies quantitatively. Nonetheless, as shown in Fig. 4, the onset of this relaxation mode for the planar oriented molecules appears at higher frequency than for the homeotropic orientation.

We conclude that $\varepsilon_{\parallel}$ was measured for the homeotropic orientation while $\varepsilon_{\perp}$ was measured for the planar orientation. This suggests a large degree of alignment of these nematic liquid crystal molecules on the mica, and confirms the conclusions from birefringence measured using optical interferometry. In principle, by using an apparatus of wider frequency range than was available to us, it would be possible to study in detail this high-frequency relaxation mode. Film thickness could be changed continuously and one could study confinement effects on molecular reorientation times of oriented confined liquid crystals.

Figure 7 compares the frequency dependence of the responses when the magnitude of the applied ac field was increased above the level of 0.1 V_{RMS}. One observes no change in the intensity of the low-frequency peak; this agrees with the hypothesis of the Helmholtz double layer. On the other hand, the intensity of the high-frequency peak increased. This peak reflects orientational polarizability of individual 5CB molecules. It is known that the static dielectric constant of 5CB is 19.7 for $\varepsilon_{\parallel}$ and 6.7 for $\varepsilon_{\perp}$. Therefore, molecules with director parallel to the electric field contribute more strongly to $C''(\omega)$ and it is reasonable that the intensity of relaxation increases with the magnitude of applied voltage.

D. Dielectric responses under shear

A unique capability of employing dielectric spectroscopy within a surface forces apparatus is to explore changes of dielectric response under an accompanying shear field. Recent studies, utilizing x-ray probes in conjunction with the surface forces apparatus, show that both confinement and shear can enhance the nematic order of liquid crystals.[9] One could study the competition between surface alignment, film thickness, and flow on molecular reorientation rates using an apparatus spanning a higher frequency range than was available to us.

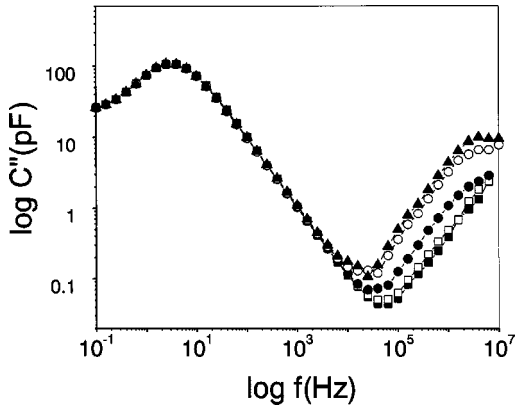

FIG. 7. Dielectric loss responses obtained with various applied ac voltages to a film of homeotropic orientation (27 Å thick). No difference was observed at $f < 10^3$ Hz, where responses are attributed to interface polarization. The intensity of the high-frequency peak corresponding to the orientational polarizability of 5CB molecules increased in intensity with increasing voltage. Applied voltages are 0.1 V_{rms} (closed squares), 0.5 V_{rms} (open squares), 1.0 V_{rms} (closed circles), 1.5 V_{rms} (open circles), and 2.0 V_{rms} (closed triangles).

Watanabe *et al.* recently investigated the effect of flow on the dielectric response of nematic liquid crystals of macroscopic thickness.[24] At temperatures corresponding to the isotropic phase, $\varepsilon^{*}(\omega)$ was unaffected by slow shear flow at shear rate $\dot{\gamma} \ll f_{\mathrm{peak}}$. However, in the nematic phase, the ε'' peak broadened on the high frequency side and the peak height, reflecting the terminal relaxation intensity, decreased. In contrast, flow did not alter the longest relaxation time, defined as $1/2\pi f_{\mathrm{peak}}$.

In Fig. 8, the dielectric response in the presence of shear is compared to the case of no shear. It was measured with a homeotropically oriented film of thickness 27 Å under dc bias of 25 V_{RMS}. Shear amplitude was 5400 Å at 1 kHz. The resulting shear rate was huge, $\dot{\gamma} \approx 10^6\ \mathrm{s}^{-1}$, but no differences in the dielectric spectrum show up when this is plotted on a log–log scale. However, when we normalize the dielectric loss under shear by the data obtained without shear (see inset of Fig. 8), a 15% increase is apparent, only at $f_{\mathrm{dielectric}} = f_{\mathrm{shear}}$. Similar experiments were also performed at different shear amplitudes and frequency. The magnitudes of the deviation of dielectric response never exceeded the level illustrated in the inset of Fig. 8. Deviations always occurred only at $f_{\mathrm{dielectric}} = f_{\mathrm{shear}}$ but a shear-induced depression of dielectric response was observed in the absence of dc bias. The relation between applied shear and the corresponding changes of dielectric loss response is not clear at present but may reflect some kind of resonance between the shear motion and the motions of ions under the electric field such that resonance occurs when the shear frequency matches the electric frequency. Further study is needed to clarify this problem.

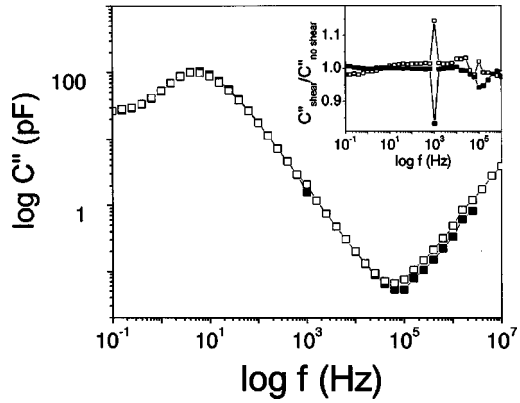

FIG. 8. Dependence on high shear rate for ultrathin films in the homeotropic orientation (27 Å thick) under 25 V dc bias (open squares) and under 0 dc bias (closed squares). The shear amplitude was 5400 Å and 2700 Å in the two cases, respectively. The frequency was 1 kHz, which corresponds to an effective shear rate of $-10^6\ \mathrm{s}^{-1}$. The out-of-phase capacitance, $C''(f)$, is plotted on log–log scales against ac frequency (f). No difference can be detected on log–log scales. In the inset, the dielectric loss obtained during shear is normalized by the data obtained in the same experiment without shear. At the shear frequency of 1 kHz, shear-induced *enhancement* was observed in the presence of dc bias, while shear-induced *depression* was observed at 1 kHz in the absence of dc bias.

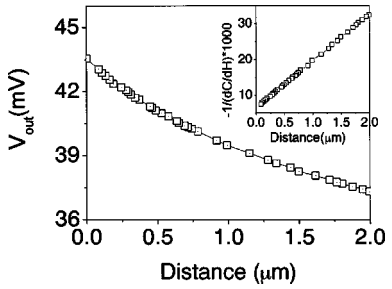

FIG. 9. The voltage output from a lock-in amplifier is plotted as a function of distance measured interferometrically by FECO fringes. In the inset, the inverse of the derivative of capacitance, $C(H)$, is plotted as a function of the distance H, and the linear relation expected from Eq. (5) is confirmed. The voltage was applied to the sputtered silver layers on the backsides of the mica sheets. Mica thickness was 4 μm and input signal was 1 V at 10 kHz.

ACKNOWLEDGMENT

This work was supported by the U.S. Department of Energy, Division of Materials Science under Award No. DEFG02-91ER45439, through the Frederick Seitz Materials Research Laboratory at the University of Illinois at Urbana-Champaign.

APPENDIX: USE OF CAPACITANCE TO MEASURE FORCE–DISTANCE PROFILES

The use of capacitance to measure surface–surface separation and force–distance profiles within a surface forces apparatus was pioneered by Frantz and co-workers.[25] Here we describe its implementation in the setup of this laboratory. A crossed-cylinder geometry is equivalent to a sphere against a flat. Whereas the capacitance between two parallel plates takes the well-known form $C=\varepsilon_o\varepsilon A/H$ (where ε_o is the vacuum permittivity, ε is the dielectric constant of the media, A is the surface area, and H is the distance between plates), the capacitance between a sphere and plate obeys a different relation. As reviewed by Georges *et al.*,[26] the approximate relation between the capacitance and the separation is given as

$$C(H)=2\pi\varepsilon R[\ln(R/H)+1.843], \tag{A1}$$

where R is the radius of curvature and H is the distance of closest approach. Therefore, the inverse of the derivative of $C(H)$ is linearly proportional to H.

Just as for the measurements of frequency-dependent dielectric response, the input voltage was kept small to minimize the attractive forces between the oppositely charged electrode surfaces. This force is given by[25]

$$F=dU/dH=(1/2)V^2dC/dH, \tag{A2}$$

where U is the energy stored by the capacitor of capacitance C and H is the distance between two plates, so that, for Eq. (A1),

$$F=-V^2\pi\varepsilon(R/H). \tag{A3}$$

When the applied voltage is 1 V, the resulting attractive force between opposed mica sheets is then only 50 nN for a typical mica thickness of 3 μm. For measurements in our surface forces apparatus (SFA) using our typical spring constant of 1000 $\mathrm{N\,m}^{-1}$ for displacements in the direction normal to the surfaces, this modest 50 nN force can induce only 0.5 Å change in separation when no force resists this displacement.

We used the bridge method to measure capacitance. Capacitor pairs were chosen to maximize sensitivity to changes in the surface separation for the mica thickness. In Fig. 9, measurements made within a surface forces apparatus are shown. Voltage was applied to the sputtered silver layer on the backside of the mica. Mica thickness was 4 μm and the input signal was 1 V at 10 kHz (thinner mica would have given better sensitivity). The output voltage in the mica–mica contact was 43 mV. In Fig. 9, voltage from a lock-in amplifier is plotted as a function of mica–mica separation deduced from FECO fringes obtained in optical interferometry. The inset shows the inverse of the derivative of $C(H)$ plotted against distance. As expected from Eq. (A1), the relationship is linear.

This distance measurement technique using capacitance was further employed to measure surface forces. As described in detail elsewhere,[27] piezoelectric bimorphs can be employed to control the separation between surfaces within a SFA. In brief, the top surface is held fixed in space and the bottom surface, fixed to a double cantilever spring comprised of two piezoelectric bimorphs, is moved in the normal direction. When we applied periodic triangular-shaped deformations as shown in the top panel of Fig. 10, the surfaces tended to approach one another and separate at constant velocity. One can control the input voltage and frequency so that the surfaces move with a desired speed. The middle panel of Fig. 10 shows, synchronized in time, the voltage output from the capacitance unit. The bottom panel of Fig. 10 shows the surface–surface separation calculated from this time-dependent voltage output. Surfaces approach one an-

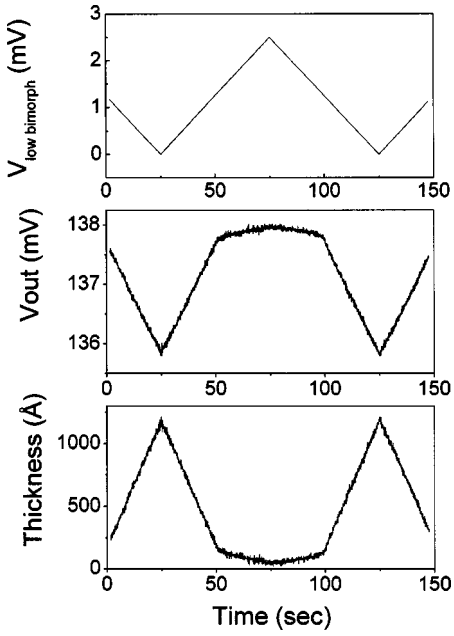

FIG. 10. When a triangular waveform is applied to a double cantilever assembly of piezoelectric bimorphs, surfaces will come together and move apart at constant velocity provided that no surface forces interfere. (Top panel) input voltage, producing periodic force in the form of a triangular waveform. One can control the input voltage and frequency so that the surface moves with a desired speed. (Middle panel) voltage output from the capacitance measurement unit is plotted against elapsed time. (Bottom panel) the time-dependent surface separation calculated from the voltage output.

other freely at large separations where there is no opposing force, but motion is attenuated in the presence of repulsive forces.

It is easy to obtain a force–distance profile using data of this kind and the known spring constant of the double-cantilever spring unit. In Fig. 11, the sample was *cis*-polyisoprene of narrow molecular weight distribution (weight-average molecular weight $M_w = 10\,600\ \mathrm{g\,mol^{-1}}$).

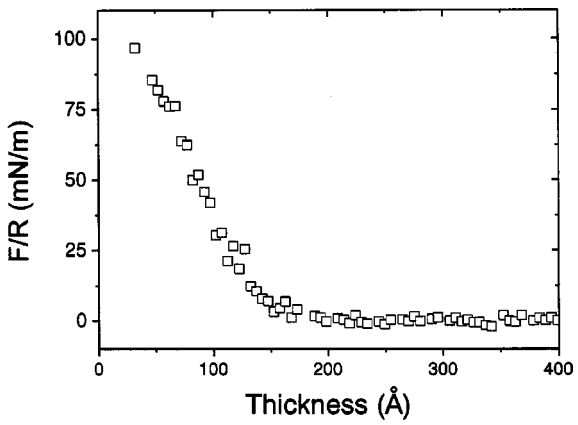

FIG. 11. Force–distance profile obtained using the data in Fig. 9 and the known spring constant of the double cantilever used to deflect the lower surface relative to the top one. Many data points at a constant film thickness were averaged. The spring constant is $1000\ \mathrm{N\,m^{-1}}$. The sample is *cis*-polyisoprene of narrow molecular weight distribution (weight-average molecular weight $M_w = 10\,600\ \mathrm{g\,mol^{-1}}$). The distance at onset of repulsive forces is about the same as measured by manually reading FECO fringes.

The force-distance profile is comparable to the one measured in the conventional fashion using FECO fringes (fringes of equal chromatic order) to measure the surface separation.[21] However, using this capacitance method, one can avoid the tedious fringe reading and much less time is required to obtain a force–distance profile. Moreover, using this method one can repeat the measurement many times easily while controlling over a wide range the speed of the approaching surfaces.

[1] J. N. Israelachvili, *Intermolecular and Surface Forces* (Academic, New York, 1990).
[2] B. Bhushan, J. N. Israelachvili, and U. Landman, Nature (London) **374**, 607 (1995).
[3] S. Granick, Science **253**, 1374 (1991); Phys. Today **52**, 26 (1999).
[4] R. G. Horn, J. N. Israelachvili, and E. Perez, J. Phys. (France) **42**, 39 (1981).
[5] V. Kitaev and E. Kumacheva, J. Phys. Chem. B **104**, 8822 (2000).
[6] M. Ruths and S. Granick, Langmuir **16**, 8368 (2000).
[7] M. Ruths, S. Steinberg, and J. N. Israelachvili, Langmuir **12**, 6637 (1996).
[8] A. Artsyukhovich, L. D. Broekman, and M. Salmeron, Langmuir **15**, 2217 (1999).
[9] C. R. Safinya, E. B. Sirota, and R. J. Plano, Phys. Rev. Lett. **66**, 1986 (1991); S. H. J. Idziak, C. R. Safinya, R. S. Hill, K. E. Kraiser, M. Ruths, H. E. Warriner, S. Steinberg, K. S. Liang, and J. N. Israelachvili, Science **264**, 1915 (1994); S. H. Idziak, I. Koltover, J. N. Israelachvili, and C. R. Safinya, Phys. Rev. Lett. **76**, 1477 (1996).
[10] I. Koltover, S. H. J. Idziak, P. Davidson, Y. Li, C. R. Safinya, M. Ruths, S. Steinberg, and J. N. Israelachvili, J. Phys. II **6**, 893 (1996).
[11] A. Dhinojwala and S. Granick, J. Chem. Phys. **107**, 8664 (1997).
[12] I. Soga, A. Dhinojwala, and S. Granick, Langmuir **14**, 1156 (1998); I. Soga, A. Dhinojwala, and S. Granick, Jpn. J. Appl. Phys., Part 1 **38**, 6118 (1999).
[13] F. M. Aliev and M. N. Breganov, Sov. Phys. JETP **68**, 70 (1989); C. Cramer, T. Cramer, F. Kremer, and R. Stannarius, J. Chem. Phys. **106**, 3730 (1997).
[14] L. M. Blinov and V. G. Chigrinov, *Electro-Optic Effects in Liquid Crystal Materials* (Springer, New York, 1994).
[15] W. H. De Jeu, *Liquid Crystals* (Academic, New York, 1978); A. R. Noble-Luginbuhl, R. M. Blanchard, and R. G. Nuzzo, J. Am. Chem. Soc. **122**, 3917 (2000).
[16] K. Takano and M. Iwamoto, Electron. Commun. Jpn., Part 2: Electron. **80**, 40 (1997); H. Koezuka, H. Kanegae, H. Ono, and K. Shibayama, J. Appl. Phys. **53**, 496 (1982).
[17] H. Mada and M. Ryuzaki, Jpn. J. Appl. Phys., Part 1 **34**, L1134 (1995); S. Murakami, H. Iga, and H. Naito, J. Appl. Phys. **80**, 6396 (1996); M. Imai, H. Naito, M. Okuda, and A. Sugimura, Mol. Cryst. Liq. Cryst. **259**, 37 (1995); B. O. Myrvold and J. Coles, *ibid.* **259**, 75 (1995); C. Colpaert, B. Maximus, and A. De Meyere, Liq. Cryst. **21**, 1 (1996); **21**, 133 (1996).
[18] A. J. Leadbetter, R. M. Richardson, and C. N. Colling, J. Phys. Colloq. **36**, C1 (1975).
[19] G. Pelzl and A. Hauser, Phase Transitions **37**, 33 (1991); P. P. Karat and N. V. Madhusudana, Mol. Cryst. Liq. Cryst. **36**, 51 (1976); R. G. Horn, J. Phys. (France) **39**, 105 (1978); A. G. Chmielewski, Mol. Cryst. Liq. Cryst. **132**, 339 (1986); H. Kneppe, F. Schneider, and N. K. Sharma, Ber. Bunsenges. Phys. Chem. **85**, 784 (1981); J. Constant and E. P. Raynes, Mol. Cryst. Liq. Cryst. **62**, 115 (1980); P. Panizza, P. Archambault, and D. Roux, J. Phys. II **5**, 303 (1995).
[20] J. Van Alsten and S. Granick, Phys. Rev. Lett. **61**, 2570 (1988); J. Peachey, J. Van Alsten, and S. Granick, Rev. Sci. Instrum. **62**, 463 (1991).
[21] Y.-K. Cho, H. Watanabe, and S. Granick, J. Chem. Phys. **110**, 9688 (1999).
[22] J. S. Patel, T. M. Leslie, and J. W. Goodbye, Ferroelectrics **59**, 137 (1984).
[23] S. A. Rozanski, R. Stannarius, H. Groothues, and F. Kremer, Liq. Cryst. **20**, 59 (1996).
[24] H. Watanabe, T. Sato, M. Hirose, K. Osaki, and M. L. Yao, Rheol. Acta **37**, 519 (1998); **38**, 100 (1999).
[25] P. Frantz, N. Agrait, and M. Salmeron, Langmuir **12**, 3289 (1996); P. Frantz, A. Artsyukhovich, and R. W. Carpick, *ibid.* **13**, 5957 (1997).
[26] C. Boyer, F. Houze, A. Tonck, J.-C. Loubet, and J.-M. Georges, J. Phys. D **27**, 104 (1994).
[27] A. Dhinojwala and S. Granick, J. Chem. Soc., Faraday Trans. **92**, 619 (1996).